

ELECTRONIC SUPPLEMENTARY INFORMATION

Freestanding Laser-Induced Two Dimensional Heterostructures for Self-Contained Paper-based Sensors

Flavio Della Pelle^{a,b}, Qurat Ul Ain Bukhari^{a,b}, Ruslán Alvarez Diduk^b, Annalisa Scroccarello^a, Dario Compagnone^{a,*}, Arben Merkoçi^{b,c,**}

^a Faculty of Bioscience and Technology for Food, Agriculture and Environment, University of Teramo, Campus "Aurelio Saliceti" Via R. Balzarini 1, 64100, Teramo, Italy

^b Nanobioelectronics & Biosensors Group, Catalan Institute of Nanoscience and Nanotechnology (ICN2), CSIC and BIST, Campus UAB, Bellaterra, Barcelona, Spain.

^c ICREA Institució Catalana de Recerca i Estudis Avançats, Barcelona, Spain

E-mail: * dcompagnone@unite.it (D. Compagnone); ** arben.merkoci@icn2.cat (A. Merkoçi)

TABLE OF CONTENTS

Supplementary Figures

Figure S1. Pictures of sensor fabrication steps	2
Figure S2. Visible spectra, pictures, and micrographs of the 4 liquid phase exfoliated TMDs	3
Figure S3. SEM micrographs and EDX mapping of the only-rGO film and sensor	4
Figure S4. XPS analysis for GO and rGO films	5
Figure S5. Cyclic voltammograms obtained with the full set of sensors in phosphate buffer, $[\text{Fe}(\text{CN})_6]^{3-/4-}$ and $[\text{Ru}(\text{NH}_3)_6]^{2+/3+}$	6
Figure S6. DP and CAT differential pulse voltammograms and H_2O_2 hydrodynamic amperometry obtained with the full set of sensors.	7
Figure S7. Differential pulse voltammetry currents of consecutive measures of DP and CAT	8
Figure S8. Differential pulse voltammograms in SCF and amperometric curves in fetal bovine serum	9

Supplementary Tables

Table S1. Real sample analysis data	10
Table S2. State of the art of TMDs combined with laser-induced graphenic structures	11

SUPPLEMENTARY FIGURES

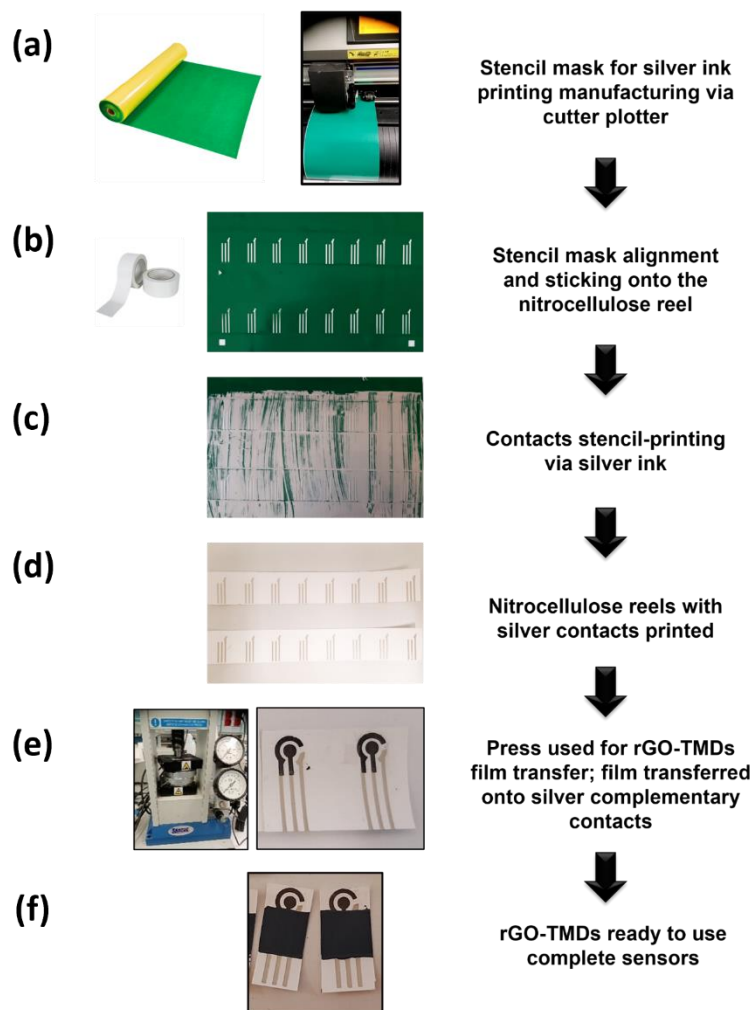


Fig. S1 Pictures of the sensor components and their main fabrication steps. **(a)** Self-adhesive vinyl reel and its molding with cutter-plotter to obtain stencil masks for silver-ink printing of the sensor contacts. **(b)** Nitrocellulose reel and stencil mask alignment and sticking onto the same. **(c)** Stencil-printing of the sensors contacts, this step is performed by squeegeeing the silver ink onto the stencil mask adhered to the nitrocellulose reel; the mask is removed after silver contacts curing. **(d)** Nitrocellulose reels with printed silver contacts; on this substrate occurs the alignment of the complementary nanostructured film before the transfer by pressure. **(e)** Hydraulic press used for the transfer of nanomaterial films, and the film transferred onto the silver complementary contacts onto the nitrocellulose support; this step aims to create the contact between the sensing material and the potentiostat used for the measurements. **(f)** Complete sensors. The electrochemical cell is composed of the working and counter electrodes of the same material (the one of the transferred film), and a pseudo-reference electrode of silver.

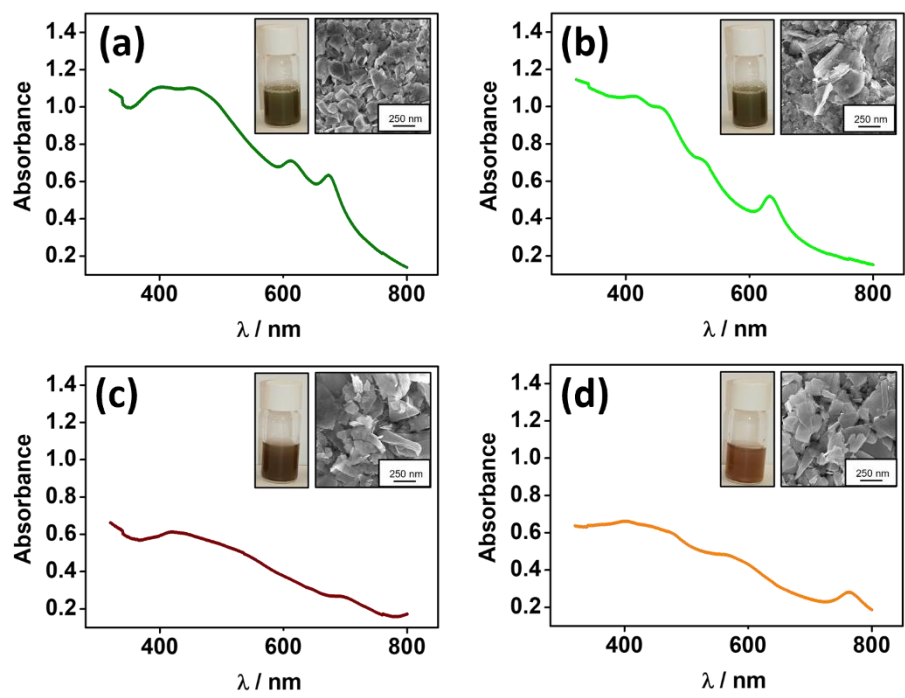


Fig. S2 Absorbance spectra of the MoS₂ (a), WS₂ (b), MoSe₂ (c), WSe₂ (d) water dispersions. In the insets, the picture of the TMD dispersion, and the micrograph of the filtered TMD are reported

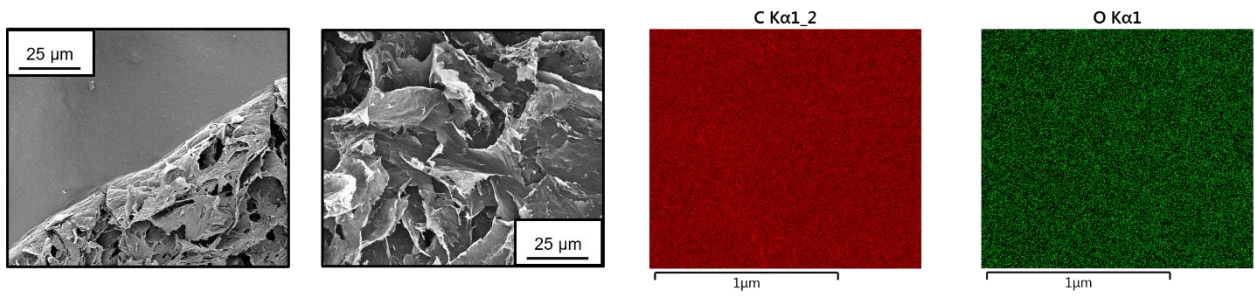


Fig. S3 SEM micrographs performed at the GO/rGO laser treatment edge and in the rGO film transferred on nitrocellulose. EDX mapping of the rGO film for the C and O elements

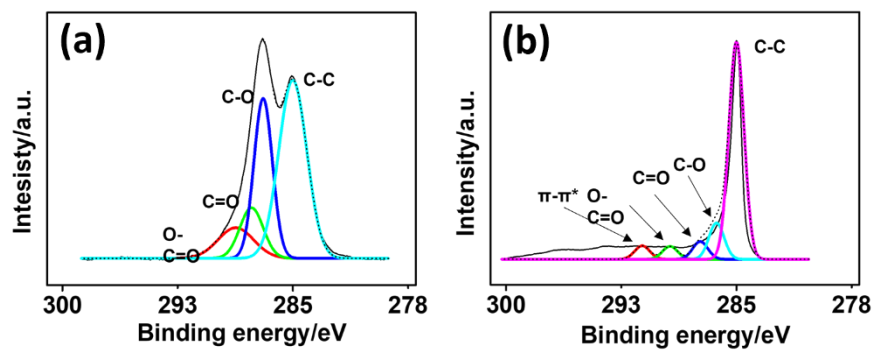


Fig. S4 XPS high-resolution spectra for the C1s of the (a) GO (before treatment) and (b) rGO (after laser treatment) films

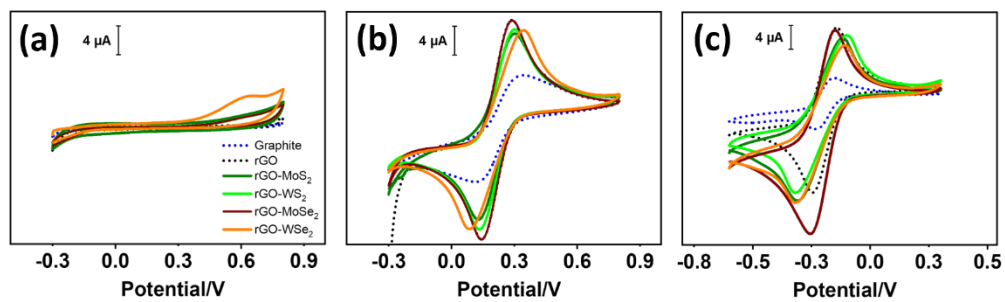


Fig. S5 Cyclic voltammograms of (a) 0.1 M phosphate buffer + 0.1 KCl, pH 7.4 (PB), (b) 1 mM [Fe(CN)₆]^{3-/4-} and (c) 1 mM [Ru(NH₃)₆]^{2+/3+} performed on a commercial graphite-SPE and with the sensors integrating the rGO and the rGO-MX₂ HTs. Scan rate 25 mV s⁻¹

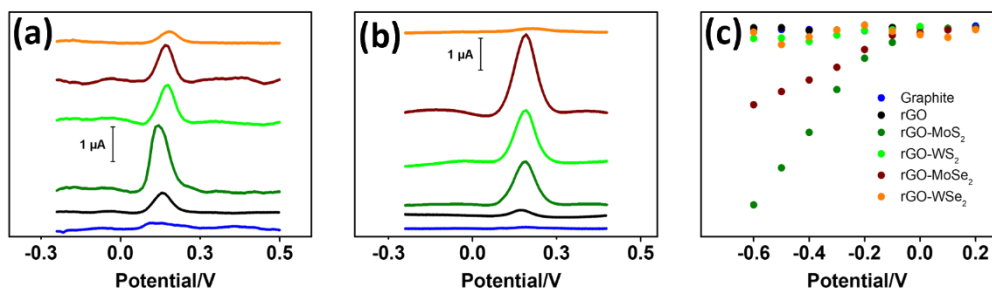


Fig. S6 Differential pulse voltammograms obtained analyzing (a) 2.5 μM dopamine and (b) 2.5 μM catechin in PB with the full set of sensors (see colorimetric legend in Figure c). DPV parameters employed: pulse width 50 ms, modulation amplitude 50 mV, scan rate 25 mV s⁻¹. (c) Hydrodynamic amperometry carried out with the full set of sensors for 0.1 mM H₂O₂ in PB

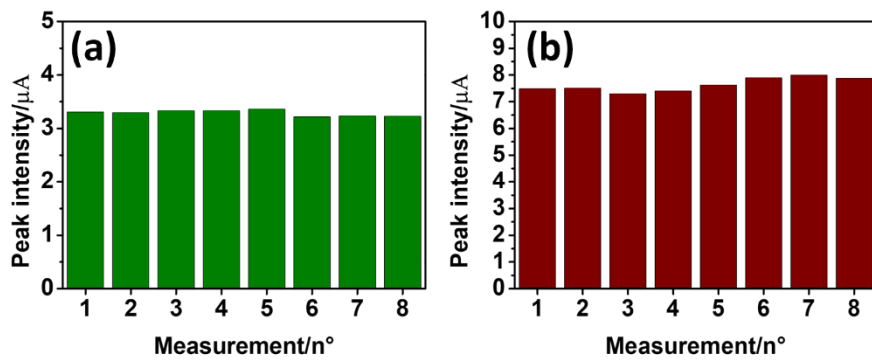


Fig. S7 Differential pulse voltammetry peak current response obtained with consecutive measures of (a) 5 μM DP and (b) 2 μM CAT in PB performed on rGO-MoS₂ and rGO-MoSe₂, respectively. DPV parameters employed: pulse width 50 ms, modulation amplitude 50 mV, scan rate 25 mV s⁻¹

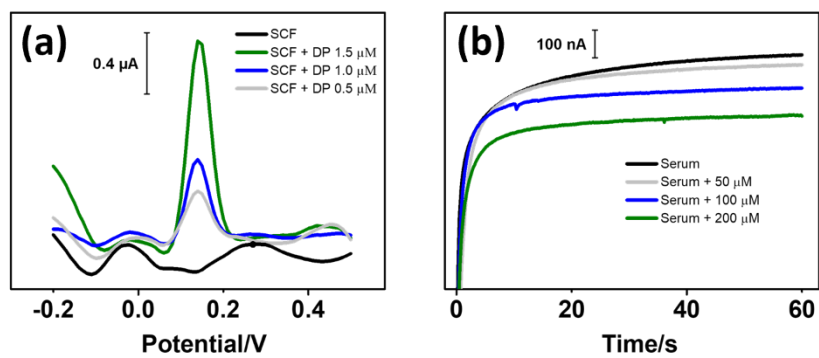


Fig. S8 (a) Differential pulse voltammograms of SCF spiked with DP at 0.5, 1.0, and 1.5 μM performed with the rGO-MoS₂ sensor. DPV parameters employed: pulse width 50 ms, modulation amplitude 50 mV, scan rate 25 mV s^{-1} . (b) Amperometric curves of fetal bovine serum spiked with H₂O₂ at 50, 100, and 200 μM performed with the rGO-MoS₂ sensor at -0.3 V

SUPPLEMENTARY TABLES

Table S1. Real sample analysis for DP (rGO-MoS₂), CAT (rGO-MoSe₂), and H₂O₂ (rGO-MoS₂). Results are expressed as mean value ± standard deviation (n = 3).

Added (μM)	Found (μM)	RSD (%)	Recovery (%)
Dopamine in SCF			
0.5	0.51±0.01	2.3	101.4
1.0	1.01±0.03	5.1	101.1
1.5	1.45±0.04	5.2	106.7
Catechin in cocoa			
0.5	0.52±0.01	2.8	104.4
1.0	1.01±0.07	6.7	100.9
1.5	1.59±0.09	5.6	106.0
H₂O₂ in serum			
50	49.6±3.4	6.8	99.1
100	105.0±6.4	6.0	105.0
200	203.0±9.3	4.6	101.5

Table S2. Components, fabrication strategy, features, and use of various TMDs combined with laser-induced graphenic structures

TMD	Graphenic material	Device	HT assembling	Practical use	Application	Ref.
MoS ₂ commercial dispersion	LIG	Supercapacitor electrodes	MoS ₂ spin-coating onto polyamide followed by laser treatment	Supercapacitors	Supercapacitors in energy conversion devices	24
MoS ₂ hydrothermal prepared	LIG	Piezoresistive sensor	MoS ₂ drop-casting onto polyamide followed by laser treatment	Strain sensor	Sensor to monitor 'deformations' of the skin	26
MoS ₂ solvothermal prepared	LIG	Gas sensor	MoS ₂ @rGO drop-casting onto LIG	NO ₂ gas sensor	NO ₂ gas sensing using stretchable devices	27
MoS ₂ commercial nanoparticles	LIG from Poly (amic acid)	Supercapacitor electrodes	MoS ₂ nanoparticles and Poly (amic acid) film formation followed by laser treatment	Flexible in-plane micro-supercapacitor	In series and in parallel interdigital electrodes for energy conversion devices.	25
MoS ₂ sonochemical dispersion	LIG	Gas sensor	MoS ₂ solution sprayed onto LIG	NO ₂ gas sensor	NO ₂ self-alarm	28
MoS ₂ WS ₂ MoSe ₂ WSe ₂ Exfoliated in water via LPE	Laser-induced reduced graphene oxide	Electrochemical paper-based sensors	rGO/MX ₂ heterostructures assembling induced by laser	Electrochemical sensing	Determination of dopamine, catechin, and H ₂ O ₂ in different food and biological samples	This work